

The Standard Free Energy of Surfactant Adsorption at Air/Water and Oil/Water Interfaces: Theoretical vs. Empirical Approaches^{1, *}

Krassimir D. Danov and Peter A. Kralchevsky

Department of Chemical Engineering, Faculty of Chemistry, Sofia University, 1 James Bourchier Blvd., Sofia, 1164 Bulgaria

Received October 7, 2011

Abstract—The standard free energy of surfactant adsorption represents the work of transfer of a surfactant molecule from the bulk of solution to an infinitely diluted adsorption layer. This quantity can be determined by non-linear fits of surface-tension isotherms with the help of a theoretical model of adsorption. Here, the models of Frumkin, van der Waals and Helfand–Frisch–Lebowitz are applied, and the results are compared. Irrespective of the differences between these models, they give close values for the standard free energy. The results from the theoretical approach are compared with those from the most popular empirical approach. The latter gives values of the standard free energy, which are considerably different from the respective true values, with c.a. 10 kJ/mol for nonionic surfactants, and with c.a. 20 kJ/mol for ionic surfactants. These differences are due to contributions from interactions between the molecules in dense adsorption layers. It is concluded that the true values of the standard free energy can be determined with the help of an appropriate theoretical model. For the processed sets of data, the van der Waals model gives the best results, especially for the determination of the standard adsorption enthalpy and entropy from the temperature dependence of surface tension. The results can be useful for the development of a unified approach to the thermodynamic characterization of surfactants.

DOI: 10.1134/S1061933X12020032

1. INTRODUCTION

The standard free energy of surfactant adsorption, ΔG° , is a surface excess of the Gibbs thermodynamic potential [1] and is widely used as a basic thermodynamic characteristic of surfactants [2–4]. The dependence of ΔG° on the surfactant chainlength for a homologous series enables one to distinguish between the contributions of the surfactant headgroups and tails into the adsorption energy [5–7]. The dependence of ΔG° on the temperature, T , along with the definition of Gibbs free energy, $\Delta G^\circ = \Delta H^\circ - T\Delta S^\circ$, allows one to determine also the standard adsorption enthalpy, ΔH° , and entropy, ΔS° . These thermodynamic parameters not only provide a quantitative characterization of surfactants, but also bring information about the molecular processes accompanying their adsorption. For example, the analysis of experimental data indicates that $T\Delta S^\circ \gg |\Delta H^\circ|$ for both ionic and nonionic surfactants, which means that the increase of entropy rather than the gain of energy determines the driving force of adsorption. This fact can be explained with the orientation of water molecules around the hydrocarbon chains in the solution that lowers the entropy of the system. Consequently the drawing of these chains out of the aqueous phase upon adsorption is accompanied by a rise of entropy [2, 3].

For nonionic amphiphiles, ΔG° can be determined from the slope of the plot of surface pressure, π_s , vs. the surfactant concentration, c , at low concentrations, at which this plot is linear (Henry region) [5]. This approach often encounters difficulties due to the slow adsorption kinetics at $c \rightarrow 0$. Because of that, Rosen and Aronson [8] proposed an empirical definition of adsorption free energy, ΔG_R° , which is easily determined by a linear fit of surface-tension data at higher concentrations. However, ΔG_R° has unclear physical meaning. Alternatively, the use of a theoretical model of adsorption allows one to determine the true value of ΔG° by a nonlinear fit of a surface-tension isotherm, which is carried out numerically. The respective systems of equations have been derived and computational procedures have been developed for both nonionic and ionic surfactants (see below).

Here, our goal is to compare the theoretical and empirical approaches to the determination of ΔG° , ΔH° and ΔS° , and to discuss the advantages and disadvantages of these approaches. In addition, our goal is to check whether the determined ΔG° , ΔH° and ΔS° are sensitive to the kind of the used theoretical model. Here, we compare the applicability of the adsorption models of Frumkin, van der Waals and Helfand–Frisch–Lebowitz, which have found numerous applications for the interpretation of surface-tension data [9–15]. Generalizations of these models to the cases of ionic surfactants and mixed sys-

¹ The article is published in the original.

* The article is dedicated to Academician Anatoly I. Rusanov on the occasion of his 80th birthday.

tems are also available [16–20]. In the present study, these models are used to determine ΔG° in the cases of air/water and oil/water interfaces, as well as of non-ionic and ionic surfactants. The results can be helpful for the development of a unified approach to the thermodynamic characterization of surfactants.

2. PHYSICOCHEMICAL BACKGROUND

Following [5, 21], let us consider the case of low adsorption of a *nonionic* surfactant at the solution's surface. In this case, the approximation for an ideal solution can be applied to both the bulk solution and adsorption layer. Setting equal the chemical potentials of the surfactant molecules in the bulk and at the surface, we obtain:

$$\mu^\circ + kT \ln c = \mu_s^\circ + kT \ln c_s, \quad (1)$$

where c and c_s are the surfactant concentrations in the bulk and in the adsorption layer; μ° and μ_s° are the respective standard chemical potentials; k is the Boltzmann constant and T is the absolute temperature. By definition, the standard free energy of surfactant adsorption is [5, 22, 23]:

$$\Delta G^\circ \equiv \mu_s^\circ - \mu^\circ. \quad (2)$$

ΔG° expresses the standard work for transfer of a surfactant molecule from the bulk of solution to an infinitely diluted adsorption layer at the surface. For the sake of brevity, hereafter we will call true standard adsorption free energy only this one, which is estimated on the basis of Eq. (2). The combination of Eqs. (1) and (2) yields [24, 5, 21, 25]:

$$\exp\left(-\frac{\Delta G^\circ}{kT}\right) = \frac{c_s}{c}. \quad (3)$$

At low surfactant concentrations, the surface pressure, $\pi_s \equiv \sigma_0 - \sigma$, obeys the Henry isotherm, viz. $\pi_s = \Gamma kT$ for $c \rightarrow 0$, where Γ is the surfactant adsorption; σ and σ_0 are the surface tensions of the solution and of the pure solvent, respectively. In addition, the adsorption can be expressed in the form $\Gamma = (c_s - c)\delta \approx c_s\delta$, where δ is a characteristic thickness of the adsorption layer, and the fact that $c_s \gg c$ for surfactants is taken into account [21]. Substituting c_s from Eq. (3), we express the surface pressure in the form:

$$\pi_s = ckT\delta \exp\left(-\frac{\Delta G^\circ}{kT}\right) \text{ for } c \rightarrow 0. \quad (4)$$

From Eq. (4), we obtain [5, 8, 26]:

$$\frac{\Delta G^\circ}{kT} = -\ln \left[\frac{1}{kT\delta} \left(\frac{d\pi_s}{dc} \right)_{c \rightarrow 0} \right]. \quad (5)$$

It is convenient to define the thickness of the adsorption layer, δ , as the length of the surfactant molecule. Because ΔG° depends on $\ln(\delta)$, the standard adsorption free energy is not too sensitive to the definition of

δ . The derivative of π_s in Eq. (5) is known also as the Traube's constant [8, 26].

Equation (5) can be used for determination of ΔG° from the slope of the $\pi_s(c)$ isotherm at low concentrations, in the Henry region. The application of this method is possible, but it needs precise measurements at low surfactant concentrations with pure substances. Because of the slow relaxation of the surface tension, σ , at low concentrations, the equilibrium σ has to be determined by extrapolation of the plot σ vs. $t^{-1/2}$ for $t \rightarrow \infty$, where t is time.

3. EMPIRICAL APPROACH FOR NONIONIC SURFACTANTS

3.1. Basic Equations

As mentioned above, there can be practical difficulties to apply Eq. (5) for determining ΔG° from the slope of the $\pi_s(c)$ isotherm at low concentrations. For this reason, Rosen and Aronson [8] proposed an empirical definition of standard adsorption free energy, ΔG_R° , which is widely used in practice, but gives a quantity that is different from ΔG° . Their approach is based on the Gibbs adsorption equation [27]:

$$d\pi_s = \Gamma kT d \ln c. \quad (6)$$

For many surfactants and interfaces, the adsorption Γ is almost constant in a relatively wide region below the critical micellization concentration (CMC), where a dense layer corresponding to adsorption $\Gamma = \Gamma_d$ is formed. Setting $\Gamma = \Gamma_d = \text{const}$, in Eq. (6) and integrating, one obtains [8]:

$$kT \ln \left(\frac{c}{\omega} \right) = \frac{1}{\Gamma_d} \pi_s + \Delta G_R^\circ \quad (\Gamma \approx \Gamma_d = \text{const}). \quad (7)$$

In Eq. (7), the integration constant is split to two parts: $kT \ln(\omega)$ and ΔG_R° . Here $\omega = \rho_w/18$ is the molar concentration of water; ρ_w (in g/L) is the mass density of water. For example, $\omega = 55.34$ M at 25°C. After Rosen and Aronson, the term ΔG_R° can be considered as a characteristic surfactant adsorption free energy, which is defined by Eq. (7).

To determine ΔG_R° , the experimental data for $\pi_s(c)$ are to be plotted as $kT \ln(c/\omega)$ vs. π_s in accordance with Eq. (7). This is illustrated in Fig. 1a with data for the nonionic surfactant Triton X-100 obtained by Janczuk et al. (the same as in Ref. [28]) and in Fig. 1b with data for *n*-alkanoic (fatty) acids from [7]. As seen, in a wide region of π_s values the experimental data comply with a straight line. In view of Eq. (7) the slope and intercept of the linear regression give, respectively, Γ_d and ΔG_R° . In the case of Triton X-100 (Fig. 1a), Γ_d is the adsorption at the CMC. In the case of fatty acids (Fig. 1b), which are below the Krafft point, Γ_d is the adsorption at the separation of fatty-acid phase (droplets or

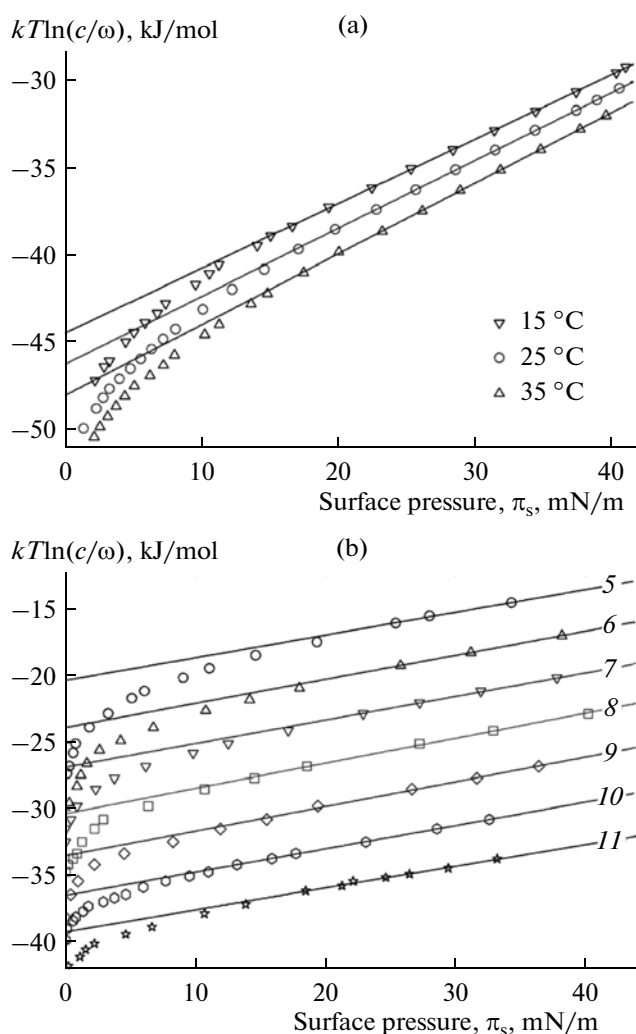


Fig. 1. Plots of experimental data for $\pi_s(c)$ in accordance with Eq. (7); ΔG_R° is determined from the intercept of the linear regression. (a) Data for Triton X-100 at three temperatures from [28]. (b) Data for *n*-alkanoic (fatty) acids, from pentanoic to undecanoic from [7]; the number of carbon atoms in each acid is denoted on the respective curve; $T = 22^\circ\text{C}$.

crystallites). As seen in Fig. 1, at the lower surface pressures, corresponding to lower surfactant concentrations, the experimental data deviate from Eq. (7), because the assumption $\Gamma = \Gamma_d = \text{const.}$ is not fulfilled at such concentrations.

Table 1. Comparison of the true and empirical adsorption energy per CH_2 group

Amphiphile	T ($^\circ\text{C}$)	$\partial \Delta G_R^\circ / \partial n_C$ (kJ/mol)	$\partial \Delta G^\circ / \partial n_C$ (kJ/mol)
<i>n</i> -alkanoic acids	22	3.12 ± 0.07	2.52
<i>n</i> -alkanols	20	3.36 ± 0.09	2.50

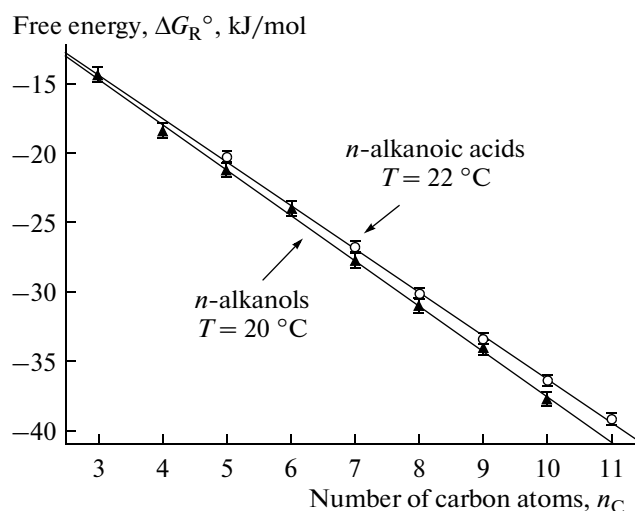


Fig. 2. Plot of ΔG_R° vs. the number of carbon atoms, n_C , for *n*-alkanoic acids at 22 °C (see Fig. 1b) and for *n*-alkanols at 20 °C; data from [7, 19].

Figure 2 shows plots of ΔG_R° vs. the number of carbon atoms, n_C , in *n*-alkanoic acids at 22 °C (for the fits in Fig. 1b), and for *n*-alkanols at 20 °C for fits of data from [7, 19] in accordance with Eq. (7). As seen in Fig. 2, the magnitude of ΔG_R° increases linearly with n_C in a qualitative agreement with the Traube's rule. The slope of each line, $\partial |\Delta G_R^\circ| / \partial n_C$, expresses the adsorption energy per CH_2 group. The $\partial |\Delta G_R^\circ| / \partial n_C$ values are markedly greater by magnitude than the $\partial |\Delta G^\circ| / \partial n_C$ values determined in [7, 19] by fits of data with the van der Waals isotherm (Table 1). The value $\partial |\Delta G^\circ| / \partial n_C = 2.50 \text{ kJ/mol} = 1.026 kT$ per molecule at 20 °C is close to the Traube's result $\ln(3) \approx 1.099 kT$. However, $\partial |\Delta G_R^\circ| / \partial n_C$ gives exaggerated (with about 30%) values of the adsorption energy per CH_2 group. For example, the value 3.36 kJ/mol for *n*-alkanols in Table 1 corresponds to 1.379 kT .

The main advantage of the approach by Rosen and Aronson [8] is that ΔG_R° can be easily determined, as illustrated in Fig. 1. The main disadvantage of this approach is that the quantity ΔG_R° is different from the standard free energy of surfactant adsorption, ΔG° , and has unclear physical meaning. Because ΔG_R° is obtained by extrapolation at $\pi_s \rightarrow 0$ (see Fig. 1), it defines the standard free energy of adsorption with respect to "a hypothetical standard state in which the surface is filled with a monolayer of surface active agent, Γ_d , at a surface pressure of zero" [8]. However, this hypothetical state is non-physical, because in reality a dense surfactant adsorption layer ($\Gamma = \Gamma_d$) has a considerable surface pressure, $\pi_s > 20 \text{ mN/m}$.

Another drawback of the empirical approach is that not always the π_s -vs.- $\ln(c)$ plot has a pronounced lin-

Table 2. Values of ΔG_R° , ΔH_R° and ΔS_R° for the nonionic surfactant Triton X-100

T (°C)	CMC (mM)	Γ_d ($\mu\text{mol}/\text{m}^2$)	$\pi_s(\Gamma_d)$ (mN/m)	$-\Delta G_R^\circ$ (kJ/mol)	ΔH_R° and ΔS_R°
Fit of data for Triton X-100 from [28]					
15	0.288	2.7	41.16	44.5	$\Delta H_R^\circ = 7.25 \pm 0.09$ kJ/mol; $\Delta S_R^\circ = 179.5 \pm 0.3$ J/(K mol)
25	0.263	2.6	40.84	46.2	
35	0.214	2.5	39.79	48.0	
Fit of data for Triton X-100 from [29]					
15	0.270	2.92	40.8	43.3	$\Delta H_R^\circ = 9.6 \pm 0.8$ kJ/mol; $\Delta S_R^\circ = 184.5 \pm 3$ J/(K mol)
30	0.224	2.75	40.4	46.0	
40	0.207	2.57	39.5	47.9	

ear portion (corresponding to $\Gamma = \Gamma_d = \text{const}$). An example is the plot for *n*-pentanoic acid in Fig. 1b. Other example is the case of *ionic* surfactants at the *oil*/water interface (see Section 7). In such cases the empirical free energy ΔG_R° cannot be reliably determined.

For ionic surfactants at the air/water interface, the π_s vs. $\ln(c)$ plots have pronounced linear portions, but the determined ΔG_R° values depend on the salt (counterion) concentration, so that they cannot be considered as characteristics of the respective surfactant. A generalization of the empirical approach to ionic surfactants, which overcomes this problem, is considered in Sect. 5.

3.2. Determination of the Standard Enthalpy and Entropy

The definition of Gibbs free energy, applied to the process of isothermal transfer of surfactant molecules from the bulk to the surface, yields:

$$\Delta G^\circ = \Delta H^\circ - T\Delta S^\circ. \quad (8)$$

As usual, ΔH° and ΔS° are the standard enthalpy and entropy of surfactant adsorption, corresponding to the changes in the respective quantities upon the transfer of a surfactant molecule from the bulk to the surface in an infinitely diluted adsorption layer.

ΔG_R° can be expressed in analogy with Eq. (8):

$$\Delta G_R^\circ = \Delta H_R^\circ - T\Delta S_R^\circ, \quad (9)$$

where ΔH_R° and ΔS_R° are the standard enthalpy and entropy of surfactant adsorption in the framework of the empirical approach [8]. To determine the latter two quantities, the data for ΔG_R° are plotted vs. T , and then ΔH_R° and ΔS_R° are determined as the intercept and slope of the ΔG_R° vs. T dependence.

To illustrate the determination of ΔG_R° , ΔH_R° and ΔS_R° and the accuracy of the obtained results, in Table 2 we compare the results from the fits of two different sets of data for Triton X-100, from [28] and [29]. ΔG_R°

is determined from the data fit with Eq. (7), see Fig. 1a, whereas ΔH_R° and ΔS_R° – from the fit of ΔG_R° vs. T with Eq. (9). From the two sets of data close values of the three investigated thermodynamic parameters are obtained. The results are close to those reported in [28]. The rather different values of ΔS_R° obtained in [29] are most probably due to a computational error.

4. THEORETICAL APPROACH FOR NONIONIC SURFACTANTS

4.1. General Relationships

Here, our goal is to determine the thermodynamic parameters ΔG° , ΔH° and ΔS° from fits of experimental data for π_s vs. c by theoretical adsorption isotherms. The models (isotherms) of Frumkin, van der Waals and Helfand–Frisch–Lebowitz (HFL) are used and the results are compared. In addition, expressions for the empirical parameter ΔG_R° are derived in the framework of each model, to clarify the reason for the difference between the values of ΔG_R° and ΔG° .

Using the expression $\Gamma = (c_s - c)\delta \approx c_s\delta$ (see Sect. 2), we can represent Eq. (3) in the form:

$$\delta \exp\left(-\frac{\Delta G^\circ}{kT}\right)c = \Gamma \quad (c \rightarrow 0). \quad (10)$$

The generalization of Eq. (10) for higher concentrations demands to take into account the interactions between the adsorbed molecules. The generalized form of Eq. (10) has the form:

$$\delta \exp\left(-\frac{\Delta G^\circ}{kT}\right)c = \Gamma f(\Gamma), \quad (11)$$

where $f(\Gamma)$ is a dimensionless function of Γ , which has the meaning of surface activity coefficient. In general, $f(\Gamma) \rightarrow 1$ for $\Gamma \rightarrow 0$ and then Eq. (11) reduces to Eq. (10). Explicit expressions for the function $f(\Gamma)$, corresponding to the aforementioned three adsorption models, are derived in Sects. 4.2, 4.3 and 4.4.

Substituting c from Eq. (11) into the Gibbs adsorption equation, Eq. (6), and integrating, we obtain the surface equation of state, $\pi_s = \pi_s(\Gamma)$, in the form:

$$\frac{\pi_s}{kT} = \Gamma + \int_0^\Gamma \hat{\Gamma} d \ln [f(\hat{\Gamma})], \quad (12)$$

where $\hat{\Gamma}$ is an integration variable. Furthermore, to obtain a theoretical expression for ΔG_R° , we substitute c and π_s from Eqs. (11) and (12) into Eq. (7):

$$\frac{\Delta G_R^\circ}{kT} = \frac{\Delta G^\circ}{kT} + \ln \left(\frac{\Gamma_d}{\omega \delta} \right) + g(\Gamma_d), \quad (13)$$

where the dimensionless function g is defined as follows:

$$g(\Gamma) \equiv \frac{1}{\Gamma} \int_0^\Gamma \{ \ln [f(\hat{\Gamma})] - 1 \} d \hat{\Gamma}. \quad (14)$$

As usual, Γ_d is the value of adsorption for the dense layer, which corresponds to the linear portion of the π_s -vs.- $-\ln(c)$ plot. For surfactants above the Krafft point, Γ_d is the adsorption at the CMC. The summary contribution of the last two terms in Eq. (13) is negative, so that $|\Delta G_R^\circ| > |\Delta G^\circ|$, both free energies being negative. The difference between them can be of the order of 10 kJ/mol; see below.

4.2. Frumkin Model

The Frumkin isotherm can be derived by means of statistical mechanics using a two-dimensional lattice statistics with interactions between the nearest members in Bragg–Williams approximation [30, 31]. In other words, the Frumkin model corresponds to the Langmuir model of adsorption, which is upgraded by taking into account the interactions between neighboring adsorbed molecules. Despite the use of lattice statistics that assumes localized adsorption (more appropriate for solid surfaces) the Frumkin isotherm provides very good fits of surface-tension data for liquid interfaces; see e.g. [10, 18, 31].

In the framework of the Frumkin model, the function $f(\Gamma)$ in Eq. (11) has the form [10, 18, 31]:

$$f = \frac{\Gamma_\infty}{\Gamma_\infty - \Gamma} \exp \left(-\frac{2\beta\Gamma}{kT} \right), \quad (15)$$

where Γ_∞ is the maximum possible value of the adsorption and β is a parameter that accounts for the interaction between the adsorbed surfactant molecules. For air/water interfaces, $\beta > 0$ and accounts for the van der Waals attraction between the hydrocarbon tails of the adsorbed molecules across air; for oil–water interface,

$\beta \approx 0$ [18]. The substitution of Eq. (15) into Eqs. (12) and (14) yields:

$$\frac{\pi_s}{kT} = -\Gamma_\infty \ln \left(1 - \frac{\Gamma}{\Gamma_\infty} \right) - \frac{\beta\Gamma^2}{kT}, \quad (16)$$

$$g(\Gamma_d) = -\frac{\beta\Gamma_d}{kT} - \frac{\Gamma_\infty - \Gamma_d}{\Gamma_d} \ln \left(\frac{\Gamma_\infty}{\Gamma_\infty - \Gamma_d} \right). \quad (17)$$

In addition, the substitution of Eq. (17) into Eq. (13) yields an expression for ΔG_R° .

In the framework of the Frumkin model, Eqs. (11), (15) and (16) determine the theoretical dependence $\pi_s(c)$, which can be applied to fit experimental data for nonionic surfactants and to find Γ_∞ , β and ΔG° as adjustable parameters; see Sect. 4.5.

4.3. Van der Waals Model

The van der Waals isotherm corresponds to a statistical model of two-dimensional non-ideal gas, i.e. to non-localized adsorption; see e.g. [30]. In the framework of this model, the expressions for $f(\Gamma)$ and $\pi_s(\Gamma)$ have the form [10, 18, 31]:

$$f(\Gamma) = \frac{\Gamma_\infty}{\Gamma_\infty - \Gamma} \exp \left(\frac{\Gamma}{\Gamma_\infty - \Gamma} - \frac{2\beta\Gamma}{kT} \right), \quad (18)$$

$$\frac{\pi_s}{kT} = \Gamma \frac{\Gamma_\infty}{\Gamma_\infty - \Gamma} - \frac{\beta\Gamma^2}{kT}. \quad (19)$$

The meaning of the parameters Γ_∞ and β is analogous to that in Sect. 4.2. However, the values of Γ_∞ and β obtained from fits of experimental data are different for the Frumkin and van der Waals models; see below. Combining Eqs. (13), (14) and (18), we obtain:

$$\frac{\Delta G_R^\circ}{kT} = \frac{\Delta G^\circ}{kT} - \ln \left[e\omega\delta \left(\frac{1}{\Gamma_d} - \frac{1}{\Gamma_\infty} \right) \right] - \frac{\beta\Gamma_d}{kT}, \quad (20)$$

where e is the Napier constant. Eq. (20) shows that even for non-interacting point molecules ($\beta = 0$, $1/\Gamma_\infty = 0$) there is a difference between ΔG° and ΔG_R° because of the different choice of the standard (reference) states.

In the framework of the van der Waals model, Eqs. (11), (18) and (19) determine the theoretical dependence $\pi_s(c)$, which can be applied to fit experimental data for nonionic surfactants and to find Γ_∞ , P and β as adjustable parameters; see Sect. 4.5.

4.4. Helfand–Frisch–Lebowitz (HFL) Model

The HFL model [32] also corresponds to non-localized adsorption, but it differs from the van der Waals model by the way in which the hard-core interactions are taken into account. In the framework of

the HFL model, the dimensionless function f and the surface pressure π_s are expressed in the form [13]:

$$f(\Gamma) = \frac{\Gamma_\infty}{\Gamma_\infty - \Gamma} \exp \left[\frac{\Gamma(3\Gamma_\infty - 2\Gamma)}{(\Gamma_\infty - \Gamma)^2} - \frac{2\beta\Gamma}{kT} \right], \quad (21)$$

$$\frac{\pi_s}{kT} = \Gamma \frac{\Gamma_\infty^2}{(\Gamma_\infty - \Gamma)^2} - \frac{\beta\Gamma^2}{kT}. \quad (22)$$

The meaning of the parameters Γ_∞ and β is analogous to that in Sects. 4.2 and 4.3. However, the values of Γ_∞ and β obtained from fits of experimental data with the HFL model are different from those obtained using the Frumkin and van der Waals models; see below.

Combining Eqs. (13), (14) and (21), we obtain an analogue of Eq. (20):

$$\frac{\Delta G_R^\circ}{kT} = \frac{\Delta G^\circ}{kT} - \ln \left[e\omega\delta \left(\frac{1}{\Gamma_d} - \frac{1}{\Gamma_\infty} \right) \right] - \frac{\beta\Gamma_d}{kT} + \frac{\Gamma_d}{\Gamma_\infty - \Gamma_d} \quad (23)$$

The last term in Eq. (23), which makes the difference with Eq. (20), is positive and varies between 1 and 3.

In the framework of the HFL model, Eqs. (11), (21) and (22) determine the theoretical dependence $\pi_s(c)$, which can be applied to fit experimental data for nonionic surfactants and to find Γ_∞ , β and ΔG° as adjustable parameters; see Sect. 4.5.

4.5. Fits of Data for Triton X-100 by the Three Models

Here, the above three models are tested against the same set of experimental data, viz. the data from [28] for Triton X-100 at three different temperatures. The experimental data for the surface tension, $\sigma = \sigma_0 - \pi_s$, vs. the surfactant concentration are shown in Fig. 3. The solid lines are the best fits with the theoretical models. The lines corresponding to the three different models are so close that they practically coincide in

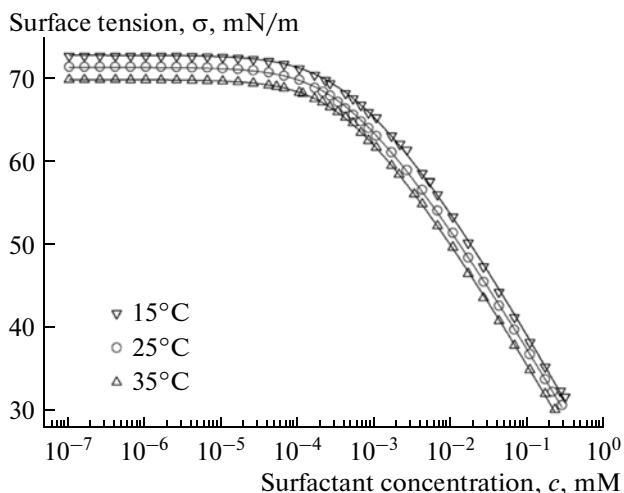


Fig. 3. Fits of data from [28] for the surface tension, σ , vs. the Triton X-100 concentration at three different temperatures. The fits by means of the Frumkin, van der Waals and HFL models (the solid lines) coincide in the framework of the graph resolution for each temperature.

Fig. 3. At each given temperature, the theoretical line was determined by minimization of the merit function:

$$\chi^2(\Gamma_\infty, \beta, \Delta G^\circ) \equiv \frac{1}{N} \sum_{n=1}^N [\sigma_{\text{th}}(c_n, \Gamma_\infty, \beta, \Delta G^\circ) - \sigma_n]^2. \quad (24)$$

Here, (c_n, σ_n) are the coordinates of the experimental points; $\sigma_{\text{th}}(c_n, \Gamma_\infty, \beta, \Delta G^\circ)$ is the theoretical dependence of the surface tension on the surfactant concentration, c_n ; the quantities Γ_∞ , β , and ΔG° are determined as adjustable parameters from the minimum of χ^2 (see Table 3). The minimal values of χ for the fits with the Frumkin, van der Waals and HFL models are,

Table 3. Parameters determined from the fits of surface-tension isotherms for Triton X-100

T (°C)	Γ_∞^{-1} (Å ²)	$\beta\Gamma_\infty/(kT)$	$-\Delta G^\circ$ (kJ/mol)	ΔH° and ΔS°
Frumkin model				
15	62.14	0.00426	34.57	$\Delta H^\circ = 4 \pm 5$ kJ/mol; $\Delta S^\circ = 140 \pm 16$ J/(K mol)
25	66.85	0.00873	36.20	
35	67.93	0.00975	37.28	
van der Waals model				
15	47.30	0.148	35.31	$\Delta H^\circ = -5.20 \pm 0.09$ kJ/mol; $\Delta S^\circ = 104.5 \pm 0.3$ J/(K mol)
25	51.91	0.530	36.36	
35	52.85	0.575	37.40	
Helfand–Frisch–Lebowitz (HFL) model				
15	33.74	1.42	34.96	$\Delta H^\circ = -7 \pm 8$ kJ/mol; $\Delta S^\circ = 96 \pm 30$ J/(K mol)
25	36.91	1.66	36.42	
35	38.76	2.30	36.87	

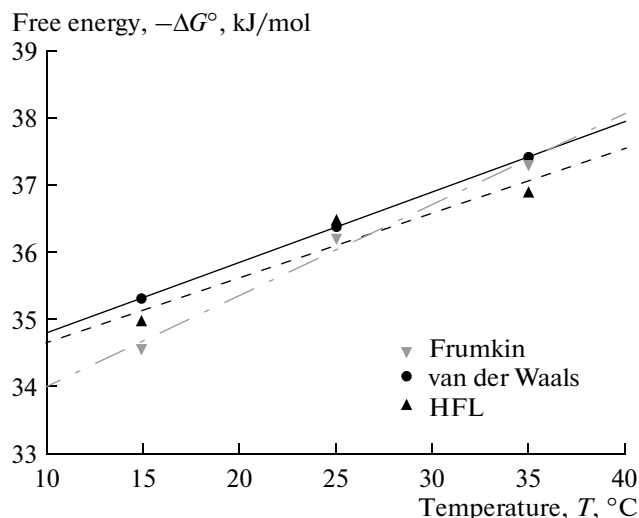


Fig. 4. Plot of the standard adsorption free energy, ΔG° , vs. temperature, T , for Triton X-100; comparison of data from Table 3 obtained by means of three different adsorption models. In accordance with Eq. (8), the standard enthalpy and entropy, ΔH° and ΔS° , are determined from the intercept and slope of the linear regressions.

respectively, $\chi_{\min} = 0.24, 0.13$ and 0.15 mN/m. Because χ_{\min} characterizes the deviation of the theoretical curves from the experimental points, its small values indicate that the fits with the three models are excellent and the differences between the three theoretical curves are really very small, as mentioned above. For all three models we used the same value for the thickness of the adsorption layer in Eq. (11), viz. $\delta = 3$ nm, which is close to the length of the Triton X-100 molecule.

The minimum of the merit function $\chi^2(\Gamma_\infty, \beta, \Delta G^\circ)$ is well pronounced, which allowed us to reliably determine the values of the three variables that correspond to the best fit. The minimum of this function is the most shallow along the direction of variation of β , and consequently, β is determined with the lowest accuracy among the three adjustable parameters. For this reason, more complex models in which β is a function depending on two (or more) additional parameters [13] are practically inapplicable, because additional parameters cannot be reliably determined from such fits.

For each separate model, the values of ΔG° are plotted vs. the temperature T and fitted with a linear regression, which gives ΔH° and ΔS° as intercept and slope; see Fig. 4 and Eq. (8). The obtained values of ΔH° and ΔS° are also given in Table 3 for each of the three models.

4.6. Discussion

First of all, it is important to note that the values of ΔG° obtained from fits of the same data with the three

different models are very close (Table 3). This result can be explained with the fact that the parameter ΔG° is related to the behavior of adsorption at low surfactant concentrations, and the three considered models reduce to the Henry isotherm, Eq. (4), at $c \rightarrow 0$. We could expect that all adsorption models that reduce to the Henry isotherm at $c \rightarrow 0$ (these considered here, as well as the Langmuir and Volmer models [23, 33]), should give close values of ΔG° . This result overcomes one of the main doubts related to the use of fits with theoretical models for determining ΔG° , viz. that different models might give different values of ΔG° . The value of ΔG° determined in this way has the true physical meaning of this quantity corresponding to its definition, Eq. (2). The empirically determined parameter ΔG_R° is with about 10 kJ/mol greater (by magnitude) from ΔG° ; compare Tables 2 and 3. Eqs. (20) and (23) indicate that ΔG_R° contains contributions from the hard-core and long-range interactions between the surfactant molecules in the adsorption layer, which are characterized by the parameters Γ_∞ and β .

Although the standard free energy, ΔG° , is not sensitive to the choice of the adsorption model, Table 3 indicates that this is not the case with the standard enthalpy and entropy, ΔH° and ΔS° . For the considered example, only the van der Waals model yields a good linear dependence (Fig. 4) and the values of ΔH° and ΔS° are determined with an excellent accuracy. For the Frumkin and HFL models, the error of ΔH° (characterized by the error of the intercept of the linear regression, see Table 3 and Fig. 4) is so large that ΔH° is not reliably determined for these two models. The obtained ΔS° is the greatest for the Frumkin model (localized adsorption), while the van der Waals and HFL models (non-localized adsorption) give closer values of ΔS° . However, the error of ΔS° (characterized by the error of the slope of the linear regression) is rather large for the Frumkin and HFL models. It should be also noted that the empirical ΔS_R° is greater than the theoretical ΔS° ; see Tables 2 and 3.

The physical meaning of the parameter Γ_∞ implies that Γ_∞^{-1} should be close to the area per surfactant molecule in a densely packed adsorption layer. For Triton X-100, the area per molecule is determined by the geometrical cross-sectional area of the polyethylene oxide chain, which on average has 9.5 ethylene oxide units. A molecular-dynamics study of polyethylene oxide (PEO) [34] shows that a PEO9 molecule has ellipsoidal form with axes $7.1 \times 9.9 \times 18.2$ Å, which corresponds to a maximal cross-sectional area of 55.2 Å² (perpendicular to the longest axis) at temperature 35°C. The latter value is the closest to $\Gamma_\infty^{-1} = 52.8$ Å² obtained by the van der Waals model at this temperature. The data in Table 3 show that the area per molecule, Γ_∞^{-1} , increases with the rise of temperature, which could be explained with temperature-dependent con-

Table 4. Comparison of the areas per molecule, Γ_{∞}^{-1} , determined in two different ways

Surfactant	Group determining Γ_{∞}	Γ_{∞}^{-1} , from molecular size (\AA^2)	Γ_{∞}^{-1} , from surface tension fits* (\AA^2)	References
Alkanols	paraffin chain	21.0	20.9	[19]
Alkanoic acids	COO ⁻	22–24	22.6	[7, 35]
SDS	SO ₄ ²⁻	30.0	30	[10, 36]
DDBS	benzene ring	35.3	35.6	[20]
CAPB	CH ₃ -N ⁺ -CH ₃	27.8	27.8	[37]
C _n TAB (<i>n</i> = 12, 14, 16)	N(CH ₃) ₄ ⁺	37.8	36.5–39.5	[11, 36]
Triton X-100	PEO9	55.2	52.8	[34] and here

* Fit by means of the van der Waals model.

SDS = sodium dodecyl sulfate; DDBS = dodecyl benzene sulfonate; CAPB = cocamidopropyl betaine, and C_nTAB = alkyl trimethyl ammonium bromide.

formational changes in the PEO headgroup of Triton X-100.

It is an empirical finding that the fits of surface tension isotherms with the van der Waals model give values of Γ_{∞}^{-1} that are practically coinciding with the geometrical cross-sectional areas of the respective molecules. This is illustrated in Table 4 with data for 9 surfactants obtained in different studies. This fact is helpful for the interpretation of data for surface tension, especially for surfactant mixtures, because the number of adjustable parameters can be essentially decreased if Γ_{∞}^{-1} is set equal to the geometrical cross-sectional area of the respective surfactant, which is known from the molecular structure. The Frumkin and HFL models give values of Γ_{∞}^{-1} , which are, respectively, larger and smaller than the geometrical cross-sectional area of the molecule; see Tables 3 and 4.

It should be noted that in the considered cases, Γ_{∞}^{-1} is treated as a constant parameter of the respective model, and is determined from the best fit of experimental data. More general thermodynamic approaches have been developed by Rusanov on the basis of the excluded volume [38–40] and excluded area [41] concepts. In the latter approach, the excluded area is a function of Γ , rather than a constant [41].

Having determined the parameters of each model, Γ_{∞} , β , and ΔG° (Table 3), we can further calculate the dependence $\Gamma(c)$ using Eq. (11) with $f(\Gamma)$ determined by one of Eqs. (15), (18) and (21). As seen in Fig. 5a, for the Frumkin isotherm the $\Gamma(c)$ dependence levels off at the higher concentrations, while $\Gamma(c)$ calculated for the van der Waals and HFL models is still increasing. We calculated also the Gibbs elasticity:

$$E_G \equiv \frac{\partial \pi_s}{\partial \ln \Gamma}. \quad (25)$$

The results are shown in Fig. 5b. For the Frumkin model, $E_G > 1000$ mN/m at the highest concentrations. Such high values of E_G are non-physical and can be attributed to the very slow variation of Γ at the higher concentrations (Fig. 5a). This behavior of the Frumkin (and Langmuir) models can be explained with the assumption for localized adsorption, which is inadequate for surfactant molecules at liquid interfaces [10]. The van der Waals and HFL models (describing non-localized adsorption) predict lower and realistic values of E_G at the higher surfactant concentrations (Fig. 5b). In the case of fatty acids, it was established that the values of E_G calculated from the van der Waals model are close to the experimentally measured E_G [7].

In summary, among the three applied theoretical models, the van der Waals model has the best performance: (i) It provides the best fit of the data for Triton X-100 as indicated by the smallest value of χ_{\min} for this model, (ii) The plot of the determined ΔG° vs. T exhibits the best agreement with a straight line (Fig. 4), so that ΔH° and ΔS° are determined with the highest accuracy from the intercept and slope (Table 3). (iii) The area per molecule Γ_{∞}^{-1} determined by this model practically coincides with the geometrical cross-sectional area determined by molecular-size considerations (Table 4). (iv) The Gibbs elasticity, E_G calculated by means of the van der Waals model has reasonable values at the higher surfactant concentrations (Fig. 5b).

5. EMPIRICAL APPROACH FOR IONIC SURFACTANTS

The empirical approach described in Sect. 3 is inapplicable to ionic surfactants, because the obtained ΔG_R° depends on the concentration of added electrolyte and cannot be considered as a characteristic of the

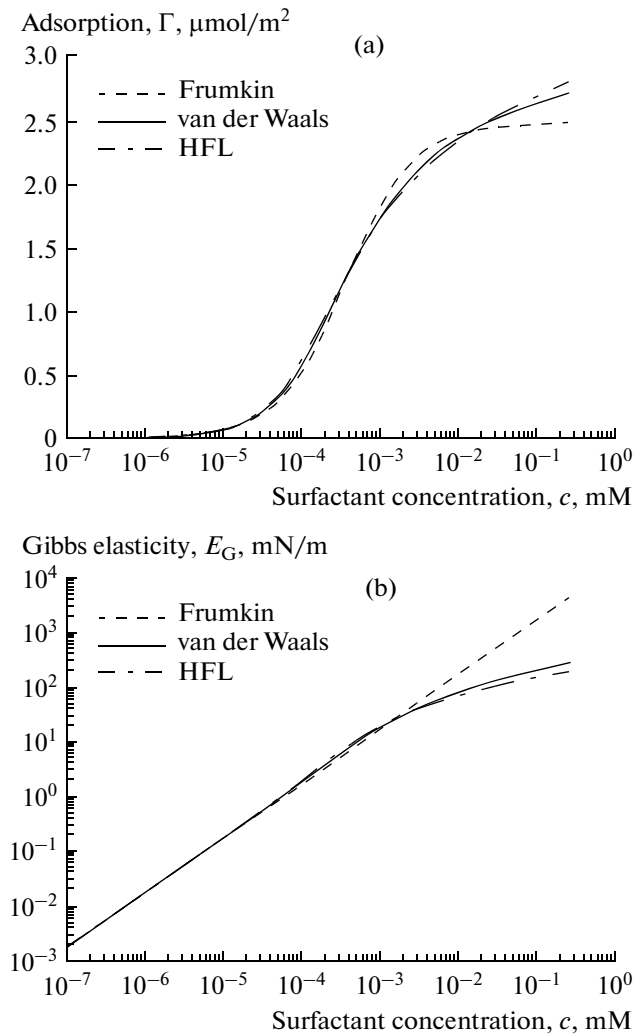


Fig. 5. Comparison of theoretical curves calculated by means of the three adsorption models using the parameters for Triton X-100 at 25°C in Table 3. (a) Surfactant adsorption, Γ , vs. surfactant concentration, c . (b) Gibbs (surface) elasticity, E_G , vs. surfactant concentration, c .

surfactant. Here, we demonstrate that this empirical approach can be generalized to the case of ionic surfactants.

For simplicity, let us consider an ionic surfactant, which is 1 : 1 electrolyte, in the presence of an additional inorganic 1 : 1 electrolyte with the same counterion. For example, this could be SDS with added NaCl (Na^+ counterion), or DTAB (dodecyltrimethylammonium bromide) with added NaBr (Br^- counterion). The Gibbs adsorption equation can be expressed in the form [18]:

$$\frac{d\pi_s}{kT} = \tilde{\Gamma}_1 d\ln(a_1) + \tilde{\Gamma}_2 d\ln(a_2) + \tilde{\Gamma}_3 d\ln(a_3), \quad (26)$$

where $a_i = c_i\gamma_{\pm}$ ($i = 1, 2, 3$) are the activities of the respective ions; c_i are bulk concentrations; the subscript 1 stands for surfactant ions; 2 – for counterions; 3 –

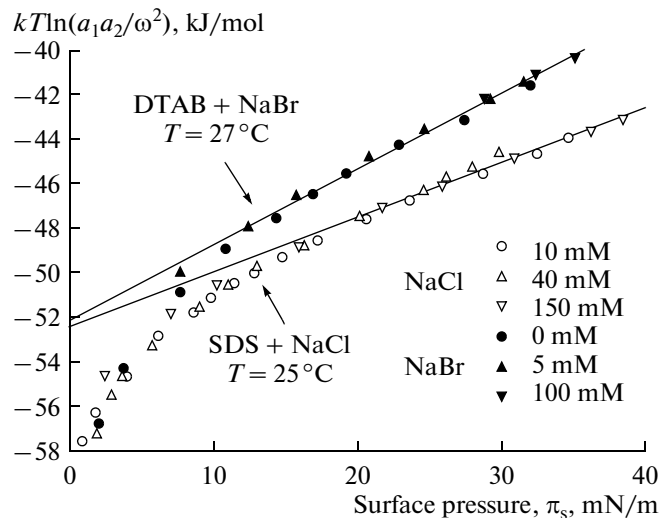


Fig. 6. Plots of experimental data for the surface tension of ionic surfactant solutions in accordance with Eq. (28); ΔG_E° is determined from the intercept of the linear regression. The data for DTAB + NaBr at $T = 27^\circ\text{C}$ are from [11, 36]; the data for SDS + NaCl at $T = 25^\circ\text{C}$ are from [36, 45].

for coions; γ_{\pm} is the bulk activity coefficient; $\tilde{\Gamma}_k$ ($k = 1, 2, 3$) is the total adsorption of the respective component, which includes contributions from both the interfacial adsorption layer and the diffuse electric double layer. The electro-neutrality of the solution leads to $\tilde{\Gamma}_2 = \tilde{\Gamma}_1 + \tilde{\Gamma}_3$. In addition, $\tilde{\Gamma}_3 \ll \tilde{\Gamma}_1, \tilde{\Gamma}_2$ at not too low surfactant concentrations see e.g. [18]. Then, $\tilde{\Gamma}_2 \approx \tilde{\Gamma}_1$ and neglecting the last term in Eq. (26), we obtain [42]:

$$\frac{d\pi_s}{kT} \approx \tilde{\Gamma}_1 d\ln(a_1 a_2). \quad (27)$$

Note that in the absence of added salt ($\tilde{\Gamma}_3 = 0$), Eq. (27) is exact.

In view of Eq. (27), the plots of π_s vs. $\ln(a_1 a_2)$ for a given surfactant at different salt concentrations collapse on a single master curve, which was established for the first time in [42]. Moreover, the plots of π_s vs. $\ln(a_1 a_2)$ are straight lines for not-too-low surfactant concentrations below the CMC, which means that a dense layer with $\tilde{\Gamma}_1 = \tilde{\Gamma}_{\text{ld}} = \text{const}$ is present. Then, integrating Eq. (27), we derive a generalization of Eq. (7) for ionic surfactants:

$$kT \ln\left(\frac{a_1 a_2}{\omega^2}\right) = \frac{1}{\tilde{\Gamma}_{\text{ld}}} \pi_s + \Delta G_E^\circ \quad (\tilde{\Gamma}_1 \approx \tilde{\Gamma}_{\text{ld}} = \text{const}), \quad (28)$$

Here, ΔG_E° is an empirical standard free energy of adsorption, which characterizes the surfactant and is independent of the concentration of added electrolyte.

In Fig. 6, data for SDS and DTAB are plotted in accordance with Eq. (28) at three different salt concentrations for each surfactant. The data at different salt concentration collapse on a single master curve. From the linear part of this curve, ΔG_E° is determined as intercept; see Eq. (28). In Table 5, the obtained values of ΔG_E° are compared with ΔG° , which is determined by fits of surface tension data in [36]—see the next section.

The advantage of the considered empirical approach based on Eq. (28), see Fig. 6, is in the simplicity of its application. The disadvantage of this approach is that it gives ΔG_E° , which is with about 20 kJ/mol different from the true standard adsorption free energy ΔG° (Table 5). Moreover, ΔG_E° has not the clear physical meaning of ΔG° , see Eq. (2). Last but not least, ΔG_E° cannot be determined in the case of ionic surfactants at an oil/water interface, for which the experimental curves have no linear portions (similar to those in Fig. 6); see Section 7.

6. THEORETICAL APPROACH FOR IONIC SURFACTANTS

The generalization of Eq. (11) for ionic surfactants reads [18]:

$$\delta \exp\left(-\frac{\Delta G^\circ}{kT} - \Phi_s\right) a_1 [1 + K_{St} a_2 \exp(\Phi_s)] = \Gamma_1 f(\Gamma_1), \quad (29)$$

where, as before, the subscripts 1 and 2 refer to surfactant ions and counterions; $\Phi_s = e|\psi_s|/(kT)$ is the dimensionless surface potential defined to be positive irrespective of whether the surfactant is anionic or cationic; e is the elementary charge; ψ_s is the dimensional surface potential, and K_{St} is the Stern constant, i.e. the constant that enters the Stern isotherm of counterion adsorption [43, 18]:

$$\frac{\Gamma_2}{\Gamma_1} = \frac{K_{St} a_2 \exp(\Phi_s)}{1 + K_{St} a_2 \exp(\Phi_s)}. \quad (30)$$

Γ_1 is the surfactant adsorption at the interface ($\tilde{\Gamma}_1$ in Eq. (26) is equal to Γ_1 plus a contribution from the diffuse layer); Γ_2 is the adsorption of counterions bound in the Stern layer. The surface charge and potential are related by the Gouy equation [44, 18]:

$$\Gamma_1 - \Gamma_2 = \frac{4I}{\kappa} \sinh\left(\frac{\Phi_s}{2}\right), \quad (31)$$

where I is the total ionic strength and κ is the Debye parameter. For a given $f(\Gamma_1)$, Eqs. (29), (30) and (31) form a system of three equations for determining Γ_1 , Γ_2 and Φ_s . This system is nonlinear and has to be solved numerically; an algorithm can be found in [18]. Finally, the surface pressure is calculated by substituting the obtained Γ_1 and Φ_s in the expression [18]:

Table 5. $\tilde{\Gamma}_{ld}$ and ΔG_E° from the linear fits in Fig. 6 with Eq. (28) and ΔG° from [36]

Surfactant	$\tilde{\Gamma}_{ld}$ (mmol/m ²)	$-\Delta G_E^\circ$ (kJ/mol)	$-\Delta G^\circ$ (kJ/mol)
SDS	4.1 ± 0.1	52.5 ± 0.2	31.1
DTAB	3.0 ± 0.1	52.2 ± 0.2	30.0

Table 6. Results from fits of surface tension isotherms by means of the van der Waals model for ionic surfactants* at the air–water interface; $T = 298$ K

Surfactant	$-\Delta G^\circ$ (kJ/mol)	$1/\Gamma_\infty$ (Å ²)	$\beta\Gamma_\infty/(kT)$	Reference
SDS	31.0	30.0	1.78	[36]
DDBS	32.9	35.6	3.42	[20]
C ₁₂ TAB	29.2	36.5	1.35	[36]
C ₁₄ TAB	35.7	36.9	0.50	[11]
C ₁₆ TAB	40.0	38.3	0.50	[11]

* $K_{St} = 6.53 \times 10^{-4}$ and 7.48×10^{-4} (mM)⁻¹ for Na⁺ and Br⁻ counterions, respectively [36].

$$\pi_s = \pi_a + 8kT \frac{I}{\kappa} \left[\cosh\left(\frac{\Phi_s}{2}\right) - 1 \right], \quad (32)$$

where the last term accounts for the contribution of the diffuse part of the electric double layer, and

$$\frac{\pi_a}{kT} = \Gamma_1 + \int_0^{\Gamma_1} \hat{\Gamma} d \ln[f(\hat{\Gamma})] \quad (33)$$

is the contribution of the adsorption layer. The above system of equations determines the theoretical dependence of surface pressure on the bulk concentrations of surfactant and salt, $\pi_s(c_1, c_3)$. The latter dependence, along with an explicit form of the function $f(\Gamma_1)$ corresponding to a given model, see e.g. Eqs. (15), (18) and (21), is used to fit experimental data for the surface tension at various concentrations of surfactant and salt. From the fit, ΔG° , K_{St} , Γ_∞ and β are determined as adjustable parameters; the latter two parameters enter Eqs. (15), (18) and (21).

Instead of ΔG° , one can determine the quantity

$$K_1 = \frac{\delta}{\Gamma_\infty} \exp\left(-\frac{\Delta G^\circ}{kT}\right) \quad (34)$$

as an adjustable parameter [10, 11, 18–20, 36]. K_1 enters the left-hand side of Eq. (29), scaled with Γ_∞ . Using Eq. (34), we calculated ΔG° from the values of K_1 determined in the cited studies with the help of the van der Waals model, Eq. (18). The results are shown in Table 6, together with the respective values of Γ_∞ and β . As seen in Table 6, the obtained values of ΔG° are not so different from those for the nonionic surfactant Triton X-100; see Table 3.

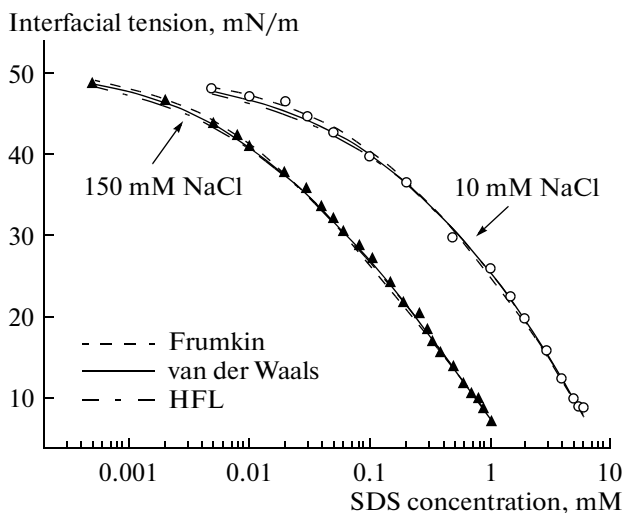


Fig. 7. Fits of data from [45] for the interfacial tension, σ , vs. the SDS concentration for *n*-hexadecane/water interface at $T = 23^\circ\text{C}$ and at two NaCl concentrations. The solid lines represent the best fits with three adsorption models denoted in the figure.

7. IONIC SURFACTANTS AT AN OIL/WATER INTERFACE

For ionic surfactants at the oil/water interface, as a rule there is no pronounced linear portion of the π_s -vs.- $\ln(a_1a_2)$ plot. In view of Eq. (27), this means that the surfactant adsorption $\tilde{\Gamma}_1$ gradually increases with the rise of surfactant concentration, instead of leveling off at a constant $\tilde{\Gamma}_{1d}$, as it is for the air/water interface. This behaviour could be explained with the intercalation of oil molecules between the surfactant tails. Upon the rise of surface pressure, π_s , these oil molecules are gradually squeezed out from the adsorption layer, so that $\tilde{\Gamma}_1$ increases. The lack of linear portion of the π_s -vs.- $\ln(a_1a_2)$ plot makes the empirical approach from Section 5 inapplicable. Only the theoretical approach from Section 6, which gives the true standard free energy ΔG° , can be used. Here, this approach is applied to determine ΔG° by processing data from [45] for the surface pressure of SDS at an *n*-hexadecane/water interface. The data are for two salt concentrations, 10 and 150 mM NaCl, at $T = 23^\circ\text{C}$; see Fig. 7.

To fit these data, we applied the models of Frumkin, van der Waals and HFL, for which the func-

tion $f(\Gamma_1)$ in Eq. (29) was substituted from Eq. (15), (18) or (21). For the Stern constant, we used the value $K_{St} = 6.53 \times 10^{-4} (\text{mM})^{-1}$ for Na^+ counterions determined in [36]. The fits with all the three models gave $\beta \approx 0$, as it is expected to be for an oil/water interface [18]. For this reason, we set $\beta \equiv 0$, and simultaneously fitted the two curves in Fig. 7 (corresponding to two different NaCl concentrations) by variation of only two parameters: ΔG° and Γ_∞ . The theoretical curves corresponding to the best fits are shown in Fig. 7 and the determined parameter values are given in Table 7. The fit with the van der Waals model is somewhat better than those with the other two models as evidenced by the smallest value of χ_{\min} in the last column of Table 7.

The values of ΔG° obtained by the three models are close but not coinciding (Table 7). All of them are greater than 31.0 kJ/mol, which is the value of ΔG° for SDS at the air/water interface (Table 6). This is an expected result, which can be explained with the van der Waals attraction between the surfactant tails and the hexadecane molecules.

The values of Γ_∞ obtained by means of the three models are very different (Table 7). The value $\Gamma_\infty^{-1} = 21 \text{ \AA}^2$ obtained by means of the HFL model is considerably smaller than the cross-sectional area of the SO_4 headgroup of SDS ($\approx 30 \text{ \AA}^2$) and is physically non-realistic. The value $\Gamma_\infty^{-1} = 34.3 \text{ \AA}^2$ obtained by means of the van der Waals model is the closest to 30 \AA^2 and seems the most realistic. The Frumkin model gives a considerably greater value of Γ_∞^{-1} (Table 7).

Having determined the parameters of the three models, we can calculate the concentration dependences of the basic physicochemical characteristics of the adsorption layer. Figure 8a shows the adsorption of SDS, Γ_1 as a function of the bulk surfactant concentration. The differences between the predictions of the three models are the greatest at the highest SDS concentrations, for which the Frumkin and HFL models predict, respectively, the lowest and highest adsorption.

Figure 8b shows the Gibbs elasticity, E_G calculated in the same way as in [10, 46]. With respect to E_G , the differences between the three models are significant. The Frumkin model predicts E_G values that are close to 1000 mN/m at the highest concentrations (just below the CMC). These values are greater than those obtained for lipid bilayers and dense protein adsorption layers, and therefore seem non-realistic for a low-molecular-weight surfactant such as SDS. From this viewpoint, the lower E_G values predicted by the van der Waals and HFL models seem physically reasonable. This can be confirmed by independent E_G measurements, which could be a task for future work.

Figure 9a shows the occupancy of the Stern layer by bound counterions, Γ_2/Γ_1 , calculated with the help of the three models. At the higher salt concentration, 150

Table 7. Parameters of the fits of the data in Fig. 7 for SDS at *n*-hexadecane/water interface

Model	ΔG° (kJ/mol)	$1/\Gamma_\infty$ (\AA^2)	χ_{\min} (mN/m)
Frumkin	35.1	49.2	0.42
van der Waals	36.2	34.3	0.27
HFL	37.2	21.0	0.35

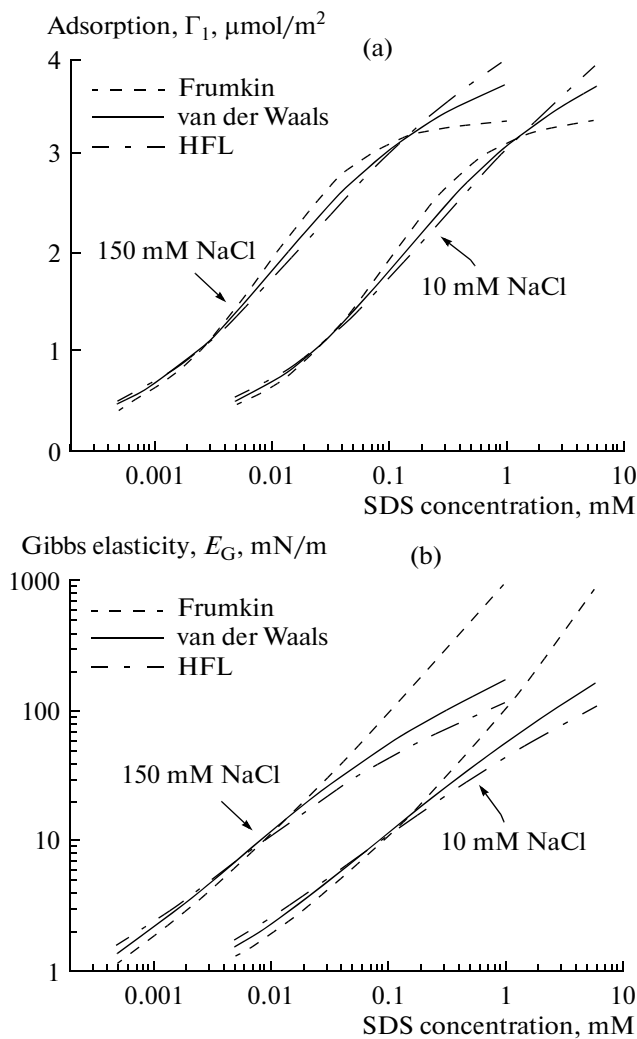


Fig. 8. Comparison of theoretical curves calculated by means of the three adsorption models using the parameters for SDS at *n*-hexadecane/water interface at $T = 23^\circ\text{C}$ in Table 7. (a) Surfactant adsorption, Γ_1 , vs. surfactant concentration. (b) Gibbs (surface) elasticity, E_G , vs. surfactant concentration.

mM NaCl, the occupancy is greater, which is to be expected. Unexpected are the large differences between the predictions of the three models, which are greater than 10% at some SDS concentrations. The greatest and the lowest occupancy are obtained, respectively, with the Frumkin and HFL models.

Figure 9b shows the magnitude of the dimensional surface electrostatic potential, $-\psi_s = (kT/e)\Phi_s$, calculated by means of the three models. As expected, the position of the predicted curves is the opposite of that in Fig. 9a: the highest occupancy of the Stern layer (for the Frumkin model) corresponds to the lowest magnitude of the surface potential. The maximum of the potential at 10 mM NaCl can be explained with the fact that the ionic surfactant (SDS) is also an electrolyte. At the lower SDS concentrations, the rise of

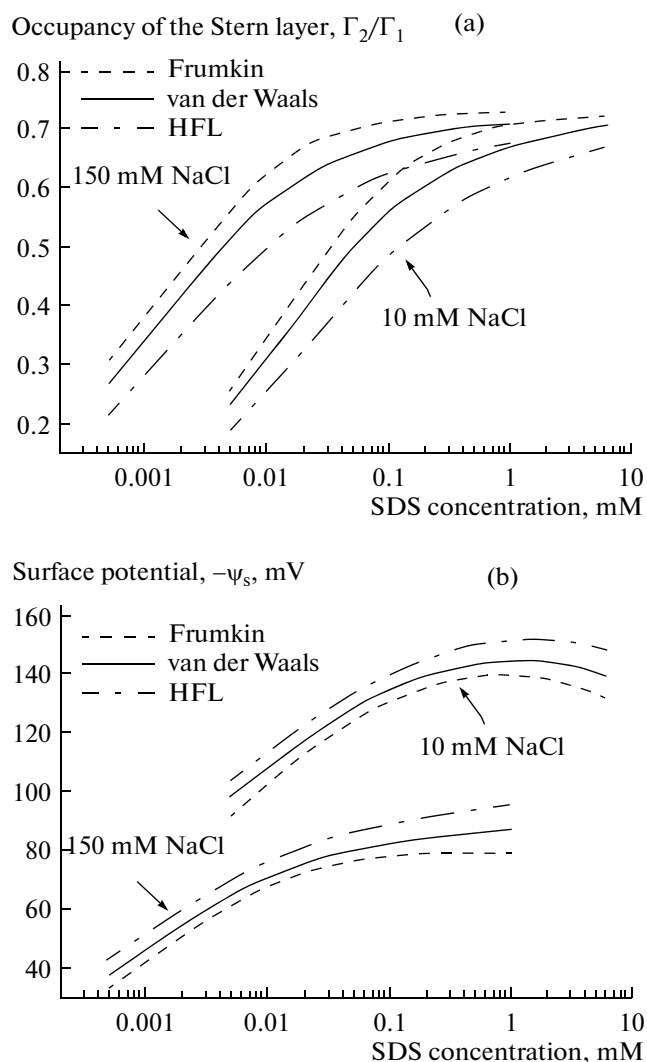


Fig. 9. Comparison of theoretical curves calculated by means of the three adsorption models using the parameters for SDS at *n*-hexadecane/water interface at $T = 23^\circ\text{C}$ in Table 7. (a) Occupancy of the Stern layer by bound Na^+ counterions, Γ_2/Γ_1 vs. the surfactant concentration. (b) Magnitude of the surface electrostatic potential, $-\psi_s$, vs. the surfactant concentration.

potential is related to the rise of the surface charge with the increase of surfactant adsorption, Γ_1 (Fig. 8a). At the higher SDS concentrations, the surfactant contributes to the Debye screening parameter, κ , and suppresses the electric double layer, so that $|\psi_s|$ decreases. In the case of 150 mM NaCl, κ is completely determined by the added salt, and because of that only the first tendency (increase of $|\psi_s|$) is present.

8. SUMMARY AND CONCLUSIONS

The concept of standard free energy of surfactant adsorption, ΔG° , was introduced by Langmuir in his interpretation of the Traube's rule [24, 25]. This quantity represents the work of transfer of a surfactant mol-

ecule from the bulk of solution into an infinitely diluted adsorption layer; see Eq. (2). By its definition, ΔG° can be determined from the slope of the plot of surface pressure vs. surfactant concentration in the Henry region at low concentrations, where this plot is linear. With the help of computer, we can determine the values of ΔG° by non-linear fits of surface-tension data by using a theoretical model of adsorption (Sect. 4). In the present study, the models of Frumkin, van der Waals and Helfand–Frisch–Lebowitz are applied, and the results are compared.

Irrespective of the differences between the three models, they give close values of ΔG° (Table 3). This result can be explained with the fact that at low surfactant concentrations the three considered models reduce to the Henry isotherm. From the temperature dependence of surface tension, the standard enthalpy and entropy of surfactant adsorption, ΔH° and ΔS° , are determined (Table 3). For the analyzed experimental data for Triton X-100, only the van der Waals model gives the values of ΔH° and ΔS° with a good accuracy (see Sect. 4.6). The theoretical approach for determining ΔG° is extended to the case of ionic surfactants at air/water and oil/water interfaces (Sects. 6 and 7).

The results from the theoretical approach are compared with those obtained by means of the most popular empirical approach for determining ΔG° [8]. The latter is based on a linear extrapolation of surface pressure data for dense adsorption layers to the limit of zero surface pressure (Fig. 1). This empirical approach, initially introduced for non-ionic surfactants, can be generalized for the case of ionic surfactants (Fig. 6). It gives values of the standard adsorption free energy, which are considerably greater (by magnitude) than the respective true values, viz. with c.a. 10 kJ/mol for nonionic surfactants, and with c.a. 20 kJ/mol for ionic surfactants (see Tables 2, 3, 5, and 6). This is due to contributions from the interactions in the dense adsorption layer to the empirically determined standard free energy; see Eqs. (20) and (23).

In conclusion, it is recommendable to determine the true values of ΔG° by nonlinear fits of surface-tension isotherms, as in Sects. 4, 6 and 7. In the present study, the best results are obtained by the van der Waals model, which provides (i) the smallest differences between theory and experiment (Sect. 4.5 and Table 7); (ii) the smallest error of the determined ΔH° and ΔS° (Table 3); (iii) physically meaningful values of the determined parameter Γ_∞ (Table 4), and (iv) reasonable values of the predicted Gibbs elasticity, E_G (Figs. 5b and 8b).

ACKNOWLEDGMENTS

The support from the National Science Fund of Bulgaria, grant No. DCVP 02/2–2009, UNION is thankfully acknowledged. The authors are grateful to Prof. Dr. Bronisław Jańczuk for providing the surface-tension data for Triton X-100 from [28] in numerical form.

REFERENCES

1. Rusanov, A.I., *Phasengleichgewichte und Grenzflächenerscheinungen*, Berlin: Akademie Verlag, 1978.
2. Couper, A., in *Surfactants*, Tadros, Th.F., Ed., London: Academic Press, 1984.
3. Durbut, P., in *Handbook of Detergents, Part A: Properties*, Broze, G., Ed., New York: Marcel Dekker, 1999.
4. Rosen, M.J., *Surfactants and Interfacial Phenomena, 3rd Edition*, New York: Wiley-Interscience, 2004.
5. Davies, J.T. and Rideal, E.K., *Interfacial Phenomena*, New York: Academic Press, 1963.
6. Kumpulainen, A.J., Persson, C.M., and Eriksson, J.C., *Langmuir*, 2004, vol. 20, p. 10935.
7. Danov, K.D., Kralchevsky, P.A., Ananthapadmanabhan, K.P., and Lips, A., *J. Colloid Interface Sci.*, 2006, vol. 300, p. 809.
8. Rosen, M.J. and Aronson, S., *Colloids Surfaces*, 1981, vol. 3, p. 201.
9. Miller, R., Fainerman, V.B., and Möhwald, H., *J. Surfactants Deterg.*, 2002, vol. 5, p. 281.
10. Kolev, V.L., Danov, K.D., Kralchevsky, P.A., Broze, G., and Mehreteab, A., *Langmuir*, 2002, vol. 18, p. 9106.
11. Valkovska, D.S., Shearman, G.S., Bain, C.D., Darton, R.C., and Eastoe, J., *Langmuir*, 2004, vol. 20, p. 4436.
12. Raut, J.S., Akella, S., Singh, A.K., and Naik, V.M., *Langmuir*, 2009, vol. 25, p. 4829.
13. Ivanov, I.B., Danov, K.D., Dimitrova, D., Boyanov, M., Ananthapadmanabhan, K.P., and Lips, A., *Colloids Surf. A*, 2010, vol. 354, p. 118.
14. Ritacco, H.A., Ortega, F., Rubio, R.G., Ivanova, N., and Starov, V.M., *Colloids Surf. A*, 2010, vol. 365, p. 199.
15. Fainerman, V.B., Aksenenko, E.V., Petkov, J.T., and Miller, R., *Colloids Surf. A*, 2011, vol. 385, p. 139.
16. Kalinin, V.V. and Radke, C.J., *Colloids Surf. A*, 1996, vol. 114, p. 337.
17. Warszyński, P., Barzyk, W., Lunkenheimer, K., and Fruhner, H., *J. Phys. Chem. B*, 1998, vol. 102, p. 10948.
18. Kralchevsky, P.A., Danov, K.D., Broze G., and Mehreteab, A., *Langmuir*, 1999, vol. 15, p. 2351.
19. Kralchevsky, P.A., Danov, K.D., Kolev, V.L., Broze, G., and Mehreteab, A., *Langmuir*, 2003, vol. 19, p. 5004.
20. Danov, K.D., Kralchevsky, S.D., Kralchevsky, P.A., Broze, G., and Mehreteab, A., *Langmuir*, 2003, vol. 19, p. 5019.
21. Shchukin, E.D., Pertsov, A.V., Amelina, E.A., and Zelenov, A.S., *Colloid and Surface Chemistry*, Amsterdam: Elsevier, 2001.

22. Wei, Y. and Latour, R.A., *Langmuir*, 2008, vol. 24, p. 6721.
23. Liu, Y., *J. Chem. Eng. Data*, 2009, vol. 54, p. 1981.
24. Langmuir, I., *J. Am. Chem. Soc.*, 1917, vol. 39, 1848.
25. Adamson, A.W. and Gast, A.P., *Physical Chemistry of Surfaces, 6th Edition*, New York: Wiley-Interscience, 1997.
26. Posner, A.M., Anderson, J.R., and Alexander, A.E., *J. Colloid Sci.*, 1952, vol. 7, p. 623.
27. Gibbs, J.W., *The Scientific Papers of J.W. Gibbs*, Vol. 1, New York: Dover, 1961.
28. Jańczuk, B., Brugue, J.M., González-Martín, M.L., and Dorado-Calasanz, C., *Langmuir*, 1995, vol. 11, p. 4515.
29. El Ghzaoui, A., Fabrègue, E., Cassanas, G., Fulconis, J.M., and Delagrangé, J., *Colloid Polym. Sci.*, 2000, vol. 278, p. 321.
30. Hill, T.L., *An Introduction to Statistical Thermodynamics*, New York: Dover, 1987.
31. Kralchevsky, P.A., Danov, K.D., and Denkov, N.D., in *Handbook of Surface and Colloid Chemistry, 3rd Edition*, Birdi, K.S., Ed., New York: Taylor & Francis, 2009, p. 197.
32. Helfand, E., Frisch, H.L., and Lebowitz, J.L., *J. Chem. Phys.*, 1961, vol. 34, p. 1037.
33. Stanimirova, R., Marinova, K., Tcholakova, S., Denkov, N.D., Stoyanov, S., and Pelan, E., *Langmuir*, 2011, vol. 27, p. 12486.
34. Lee, H., Venable, R.M., MacKerell, A.D., and Pastor, R.W., *Biophys. J.*, 2008, vol. 95, p. 1590.
35. Lunkenheimer, K., Barzyk, W., Hirte, R., and Rudert, R., *Langmuir*, 2003, vol. 19, p. 6140.
36. Christov, N.C., Danov, K.D., Kralchevsky, P.A., Ananthapadmanabhan, K.P., and Lips, A., *Langmuir*, 2006, vol. 22, p. 7528.
37. Danov, K.D., Kralchevska, S.D., Kralchevsky, P.A., Ananthapadmanabhan, K.P., and Lips, A., *Langmuir*, 2004, vol. 20, p. 5445.
38. Rusanov, A.I., *J. Chem. Phys.*, 2003, vol. 118, p. 10157.
39. Rusanov, A.I., *J. Chem. Phys.*, 2003, vol. 119, p. 10268.
40. Rusanov, A.I., *J. Chem. Phys.*, 2004, vol. 121, p. 1873.
41. Rusanov, A.I., *J. Chem. Phys.*, 2004, vol. 120, p. 10736.
42. Fainerman, V.B. and Lucassen-Reynders, E.H., *Adv. Colloid Interface Sci.*, 2002, vol. 96, p. 295.
43. Stern, O., *Ztschr. Elektrochem.*, 1924, vol. 30, p. 508.
44. Gouy, G., *J. Phys. Radium*, 1910, vol. 9, p. 457.
45. Gurkov, T.D., Dimitrova, D.T., Marinova, K.G., Bilke-Crause, C., Gerber, C., and Ivanov, I.B., *Colloids Surf. A*, 2005, vol. 261, p. 29.
46. Danov, K.D., Kolev, V.L., Kralchevsky, P.A., Broze G., and Mehreteab, A., *Langmuir*, 2000, vol. 16, p. 2942.